

A natural BH3 mimetic induces autophagy in apoptosis-resistant prostate cancer via modulating Bcl-2–Beclin1 interaction at endoplasmic reticulum

J Lian^{1,2}, X Wu^{1,3}, F He^{1,2}, D Karnak¹, W Tang¹, Y Meng¹, D Xiang^{1,2}, M Ji³, TS Lawrence¹ and L Xu^{*1}

A natural BH3-mimetic, small-molecule inhibitor of Bcl-2, (–)-gossypol, shows promise in ongoing phase II and III clinical trials for human prostate cancer. In this study we show that (–)-gossypol preferentially induces autophagy in androgen-independent (AI) prostate cancer cells that have high levels of Bcl-2 and are resistant to apoptosis, both *in vitro* and *in vivo*, but not in androgen-dependent (AD) cells with low Bcl-2 and sensitive to apoptosis. The Bcl-2 inhibitor induces autophagy through blocking Bcl-2–Beclin1 interaction, together with downregulating Bcl-2, upregulating Beclin1, and activating the autophagic pathway. The (–)-gossypol-induced autophagy is dependent on Beclin1 and Atg5. Our results show for the first time that (–)-gossypol can also interrupt the interactions between Beclin1 and Bcl-2/Bcl-xL at endoplasmic reticulum, thus releasing the BH3-only pro-autophagic protein Beclin1, which in turn triggers the autophagic cascade. Oral administration of (–)-gossypol significantly inhibited the growth of AI prostate cancer xenografts, representing a promising new regimen for the treatment of human hormone-refractory prostate cancer with Bcl-2 overexpression. Our data provide new insights into the mode of cell death induced by Bcl-2 inhibitors, which will facilitate the rational design of clinical trials by selecting patients who are most likely to benefit from the Bcl-2-targeted molecular therapy.

Cell Death and Differentiation (2011) 18, 60–71; doi:10.1038/cdd.2010.74; published online 25 June 2010

Androgen deprivation therapy is the cornerstone treatment for men with *de novo* or recurrent metastatic prostate cancer.¹ Unfortunately, it is primarily palliative, with nearly all patients progressing to an androgen-independent (AI) or hormone-refractory state, for which there is currently no effective therapy.¹ Despite several hundred clinical studies of both experimental and approved antitumor agents, chemotherapy has limited activity, with an objective response rate of <50% and no shown survival benefit.² Thus, AI disease is the main obstacle to improving the survival and quality of life in patients with advanced prostate cancer, and has been the focus of extensive studies.³ There is an urgent need for novel therapeutic strategies for the treatment of advanced prostate cancer by specifically targeting the fundamental molecular basis of progression to androgen independence and the resistance of AI disease to therapy.

Small-molecule inhibitors of anti-apoptotic Bcl-2 family members have shown promise in overcoming chemo/radioresistance in various tumor models including prostate cancer.^{4,5} (–)-Gossypol, a natural product from cottonseed, has been identified as a BH3-mimetic small-molecule pan-inhibitor of pro-apoptotic Bcl-2 family members, including Bcl-2, Bcl-xL, and Mcl-1, and induces apoptosis in various types of cancer.^{6–11} (–)-Gossypol is now in phase II and IIb

clinical trials for hormone-refractory prostate cancer and other types of cancer with promising initial results (<http://ClinicalTrials.gov>).¹² We have previously shown that (–)-gossypol sensitized AI prostate cancer cells to radiation and chemotherapy both *in vitro* and *in vivo*, and it induces apoptosis, or type I programmed cell death, by blocking the interaction of Bcl-xL with Bax and Bad in prostate cancer cells.^{13,14} However, our results also suggested that mechanisms other than apoptosis might have an important role.

Autophagy or type II programmed cell death is a major intracellular pathway for the degradation and recycling of proteins, ribosomes, and entire organelles.¹⁵ In normal cells, autophagy functions to maintain homeostasis by eliminating excessive or unnecessary proteins and injured or aged organelles. In addition, autophagy is observed under physiological conditions such as nutrient starvation, and in some pathological conditions, including myopathy, neuronal degeneration, infectious disease, and cancer.^{16–18} These findings have shed light from different directions on the role of autophagy in these diseases and on the potential of modulating autophagy as a novel therapeutic strategy. For example, MCF7 breast carcinoma cells undergo autophagic cell death rather than apoptosis after treatment with the anti-estrogen agent, tamoxifen.¹⁹ Recently, the roles

¹Division of Radiation and Cancer Biology, Department of Radiation Oncology, University of Michigan Medical School, Ann Arbor, MI 48109, USA; ²Department of Biochemistry and Molecular Biology, Third Military Medical University, Chongqing 400038, China and ³School of Chemistry and Chemical Engineering, Southeast University, Nanjing 210009, China

*Corresponding author: L Xu, Division of Radiation and Cancer Biology, Department of Radiation Oncology, University of Michigan, 4424E Med Sci I, 1301 Catherine Street, Ann Arbor, MI 48109-5637, USA. Tel: + 734 615 7017; Fax: + 734 615 3422; E-mail: liangxu@umich.edu

Keywords: (–)-gossypol; Bcl-2; Beclin1; autophagy; apoptosis

Abbreviations: AD, androgen dependent; AI, androgen independent; AVO, acidic vesicular organelles; CHX, cycloheximide; ER, endoplasmic reticulum; qRT-PCR, quantitative real-time PCR; PrEC, normal human prostate epithelial cell line; WCL, whole-cell lysate; IP, immunoprecipitation; FBS, fetal bovine serum; 3-MA, 3-methyl adenine; TEM, transmission electron microscopy; CMC, carboxymethyl cellulose

Received 16.2.10; revised 26.4.10; accepted 17.5.10; Edited by H-U Simon; published online 25.6.10

of Bcl-2 family members in autophagy have drawn more attention. The anti-apoptotic Bcl-2 family members and pro-apoptotic BH3-only proteins may participate in the inhibition and induction of autophagy, respectively. Thus, they have been proposed as dual regulators of apoptosis and autophagy.²⁰ This relatively neglected crosstalk between the core machineries regulating both autophagy and apoptosis may redefine the role of Bcl-2 family proteins in oncogenesis and tumor progression.²⁰

The BH3-mimetic compound ABT-737 induces autophagy through binding to the BH3-binding groove of Bcl-2 or Bcl-xL and releasing Beclin1, a BH3-only protein involved in autophagy.^{21,22} In our previous studies, we noticed that AI prostate cancer cells with higher level of Bcl-2 were more resistant to apoptosis induced by (–)-gossypol. However, (–)-gossypol induced similar levels of total cell death in both androgen- (AD) and AI cells; it killed AD cells mainly through apoptosis but in AI cells, the mode of cell death was not fully understood. In this study, we investigated (–)-gossypol-induced cell death in human AI prostate cancer cells *in vitro* and *in vivo*. Indeed, our data show that (–)-gossypol preferentially induces autophagy in AI prostate cancer cells that have high Bcl-2/xL and are resistant to apoptosis. Delineating the mode of cell death induced by the Bcl-2 inhibitor will not only facilitate the rational design of clinical trials, but also redefine the selection criteria for patients who will benefit the most from the Bcl-2-targeted molecular therapy.

Results

(–)-Gossypol preferentially induces apoptosis in human prostate cancer cells with low Bcl-2 but not in cells with high Bcl-2, although it is equally potent in inducing total cell death to the latter. We first verified the expression levels of Bcl-2 family proteins in a series of human prostate cancer cell lines by both western blot (Figure 1a) and quantitative real-time PCR (qRT-PCR; Figure 1b). PC-3 is AI and has much higher level of Bcl-2 and Bcl-xL than that of AD LNCaP. CL-1 is an AI clone from LNCaP and has overexpression of Bcl-2. C4-2B is another AI clone from LNCaP but has loss of Bcl-2. Bax and Bak levels were roughly equivalent between CL-1, C4-2B, and LNCaP cells, whereas PC-3 and DU-145 had lower expression of either Bak or Bax, respectively (Supplementary Figure 1). We next compared the responses of these cells with (–)-gossypol treatment in terms of total cell death (Figure 1c, Supplementary Figure 2), cell growth inhibition (Figure 1d), and apoptosis (Figures 1e–g). (–)-Gossypol induced similar levels of total cell death in these prostate cancer cell lines regardless of their expression of Bcl-2 family of proteins (Figure 1c). However, the effect of (–)-gossypol on apoptosis in these cells lines was distinctly different. Both AI lines (PC-3 and CL-1) were highly resistant to apoptosis induced by (–)-gossypol, as assayed by the sub-G1 population, caspase-3 analysis, and PARP cleavage (Figures 1e–g and Supplementary Figure 3). In contrast, LNCaP and C4-2B with low Bcl-2 were very sensitive to (–)-gossypol-induced apoptosis. DU-145 has low Bcl-2 and low Bax; its response

to (–)-gossypol was in between these two groups. Our results show that (–)-gossypol preferentially induces apoptosis in prostate cancer cells with low levels of Bcl-2 but is equally potent in inducing total cell death in cells with high levels of Bcl-2. Interestingly, the percentage of total cell death was significantly inhibited by the pan-caspase inhibitor Z-VAD in LNCaP, DU-145, and C4-2B cells (low Bcl-2 cell lines), but Z-VAD minimally affected cell death in CL-1 and PC-3 cells (Figure 1h). In addition, Z-VAD inhibited the percentage of apoptotic cells, caspase 3 activation, and PARP cleavage in all cell lines tested, but these indicators of apoptosis were low and barely detectable in PC-3 and CL-1 cells (Supplementary Figure 4). These data suggest that (–)-gossypol causes cell death by a mechanism other than apoptosis in AI prostate cancer cells with high levels of Bcl-2.

(–)-Gossypol preferentially induces autophagic cell death in AI prostate cancer cells with high levels of Bcl-2 but not in cells with low Bcl-2.

To investigate whether (–)-gossypol induced cell death is because of autophagy, we examined LC3-II conversion by immunoblotting and fluorescent microscopy in (–)-gossypol-treated prostate cancer cells. LC3-II is widely used as a marker of autophagy because its lipidation and specific recruitment to autophagosomes provides a shift from diffuse to punctate staining of the protein and increases its electrophoretic mobility on gels compared with LC3-I.²¹ Significant conversion of LC3-I to LC3-II was detected in apoptosis-resistant, AI cells with high Bcl-2 (PC-3 and CL-1) treated for 24 h with 10 μ M (–)-gossypol (Figure 2a). (–)-Gossypol-induced LC3-II conversion in PC-3 and CL-1 cells was dose and time dependent (Figures 2b and c) and was blocked by the autophagy inhibitor, 3-methyl adenine (3-MA; Figure 2a). LC3-II conversion was observed neither in the AD LNCaP cells nor the AI DU-145 and C4-2B cells with low Bcl-2, nor in normal human prostate epithelial cells. However, rapamycin induced autophagy in all cell lines except DU-145, indicating that the autophagy machinery is intact in LNCaP and C4-2B cells (Figure 2a). We also used electron microscopy to analyze (–)-gossypol-induced autophagy. We found that more autophagic vacuoles with cellular contents resembling autophagosomes appeared in (–)-gossypol-treated PC-3 and CL-1 cells compared with DMSO-treated controls (60–70% *versus* <5%; Figure 2d, black arrows).

We next examined the (–)-gossypol-induced autophagy by LC3-GFP and acridine orange staining. Recruitment of LC3-II to the autophagosomes is characterized by a punctate pattern of its subcellular localization.²¹ Autophagic cells show processing and recruitment of LC3 and appearance of red/orange acidic vesicular organelles (AVOs), which are hallmarks of autophagy.^{23,24} In CL-1 and PC-3 cells transfected with LC3-GFP, (–)-gossypol treatment induced autophagy as evidenced by a punctate pattern of green fluorescent LC3-GFP (Figure 3a, yellow arrows). Other cell lines showed very few cells containing either LC3-GFP puncta or AVOs. The DMSO control cells showed diffuse LC3-associated green fluorescence. Similar results were observed with acridine orange staining (Supplementary Figure 5A, B). The percentage of cells with the punctate

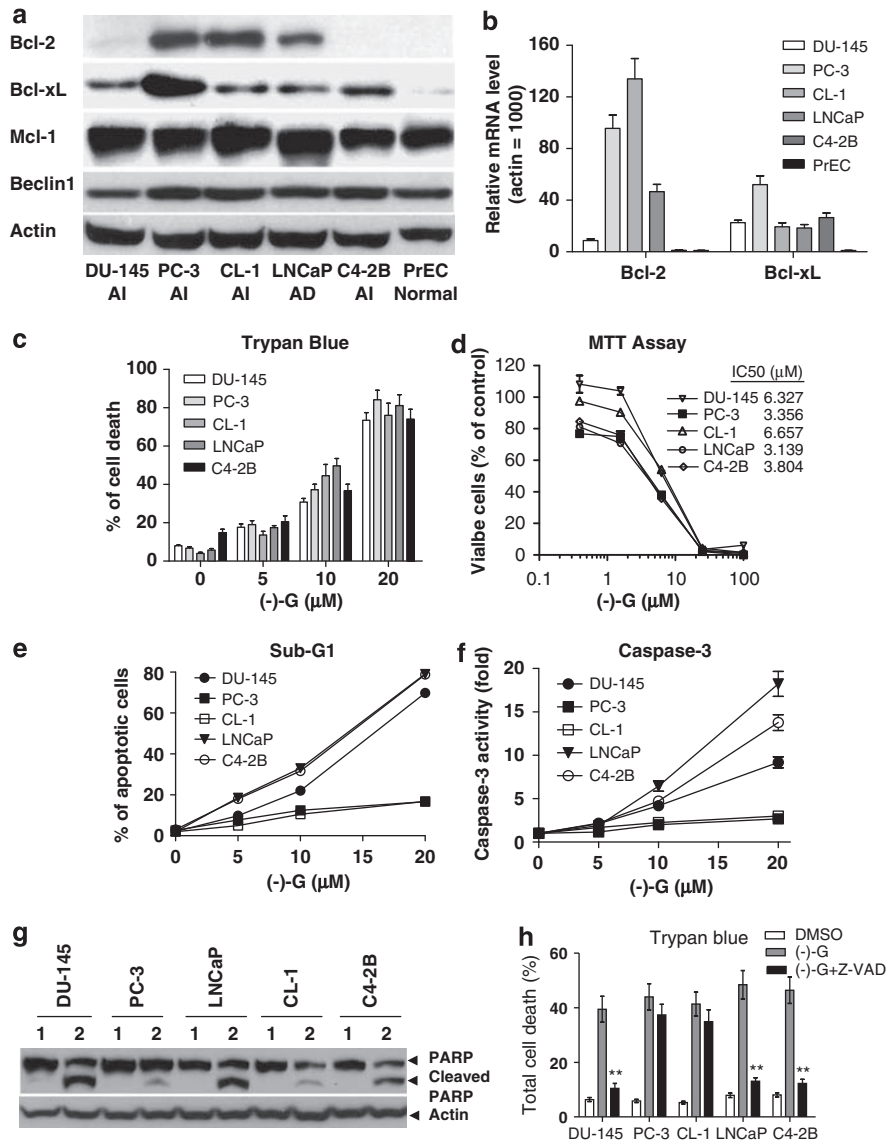


Figure 1 (-)-Gossypol preferentially induces apoptosis in human prostate cancer cells with low Bcl-2, but is equally potent in inducing non-apoptotic cell death in cells with high levels of Bcl-2. (a) Western blot analysis of the protein levels of Bcl-2, Bcl-xL, Mcl-1, and Beclin1 in prostate cancer cell lines and normal prostate epithelial cells (PrECs); (b) mRNA levels of Bcl-2 and Bcl-xL in these cells by qRT-PCR. (c) (-)-Gossypol dose-dependently induces cell death in prostate cancer cells regardless of their Bcl-2 levels. Cells (1×10^4) were seeded in a 12-well plate overnight, and then treated with different doses of (-)-gossypol. After 24 h, they were trypsinized and counted after Trypan blue staining. Data are presented as percentage of dead cells. Results are mean \pm S.D. of three independent experiments. (d) MTT-based cytotoxicity assay of (-)-gossypol in prostate cancer cells. Cells were seeded in 96-well plates and treated in triplicates. (e) (-)-Gossypol-induced apoptosis in prostate cancer cells as assayed by sub-G1 analysis. After being treated with (-)-gossypol for 24 h, the cells were fixed by ethanol, stained with PI, and analyzed by flow cytometry. (f) (-)-Gossypol-induced caspase-3 activation in prostate cancer cell lines. Cells (1×10^5) were seeded in a 12-well plate overnight and then treated with (-)-gossypol. After 24 h, caspase-3 activity was measured. (g) PARP cleavage in prostate cancer cells treated with 10μ M (-)-gossypol for 24 h. (h) After overnight culture, cells were treated with DMSO, 10μ M (-)-gossypol, or (-)-gossypol ((-)-G) combined with Z-VAD (10μ M) for 24 h. Cells were then trypsinized and counted after Trypan blue staining. Results are means \pm S.D. of three independent experiments. ** $P < 0.01$ between (-)-G and (-)-G + Z-VAD in indicated cell lines by two-way ANOVA

pattern signifying either LC3-GFP (Figure 3b) or AVOs (Supplementary Figure 5B) was significantly increased in (-)-gossypol-treated CL-1 and PC-3 cells with high Bcl-2, but not in the cells with low Bcl-2, for example, DU-145, LNCaP, and C4-2B.

The prevalence of autophagic indicators between cells that showed high versus low levels of apoptotic cell death was vastly different. As autophagy can either be a protective response or lead to cell death, we next determined whether or

not knocking down essential autophagic proteins or inhibiting autophagy with 3-MA affected cell death in CL-1 cells versus LNCaP cells. Total (-)-gossypol-induced cell death was markedly decreased in CL-1 cells either transfected with shRNAs that targeted Atg5 or Beclin1 or treated with 3-MA (Figure 3c). LNCaP cells tested in the same way were killed by (-)-gossypol at a slightly higher rate when autophagy was inhibited (Figure 3d). Collectively, these observations show that (-)-gossypol induces autophagic cell death preferentially

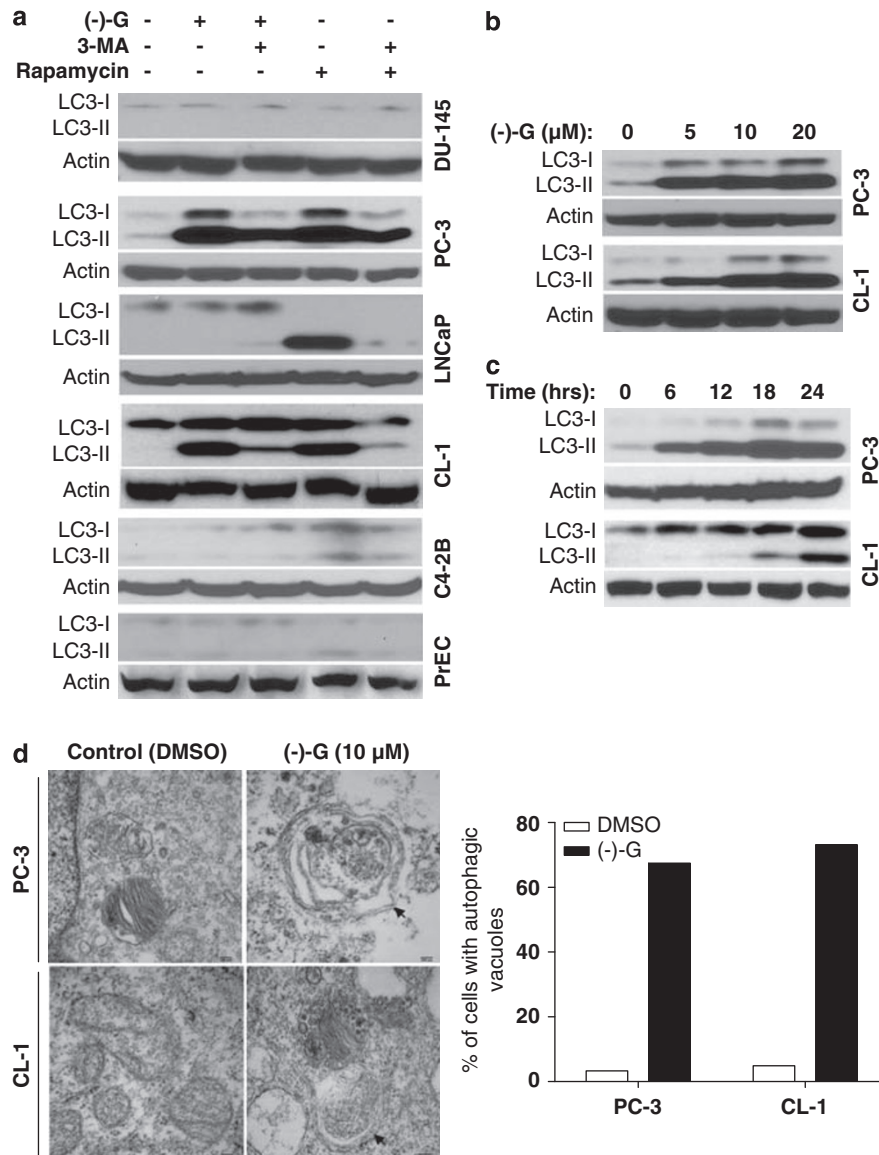


Figure 2 (-)-Gossypol preferentially induces autophagy in apoptosis-resistant prostate cancer cells with high levels of Bcl-2 but not in cells with low Bcl-2. (a) (-)-Gossypol-induced autophagy in prostate cancer cells as revealed by LC3-II conversion in western blot analysis. Cells were treated with DMSO or 10 μM (-)-gossypol for 24 h, and then lysed for western blot of LC3. 3-MA 5 mM and rapamycin 0.5 μM were used as an inhibitor and an inducer of autophagy, respectively. (b, c) Dose response (b) and time course (c) of (-)-gossypol-induced autophagy in PC-3 and CL-1 cells. (d) Representative electron microscopic images showing autophagic vacuoles with content (black arrows) after (-)-gossypol treatment. The percentage of cells with autophagic vacuoles was quantified in 50 cells each group

in all human prostate cancer cells with high Bcl-2 but not in cells with low Bcl-2.

(-)-Gossypol induces autophagy in prostate cancer cells through modulating Bcl-2–Beclin1 interaction. To investigate the mechanism of autophagy induced by (-)-gossypol, we used a co-immunoprecipitation (Co-IP) pull-down assay. IP of Beclin1 with specific antibodies pulled down Bcl-2 from whole-cell lysates (WCLs), mitochondrial fractions, and the fractions with enriched endoplasmic reticulum (ER) (Figure 4). This indicated that Bcl-2 and Beclin1 were bound to each other at both mitochondria and ER in the cells, consistent with previous studies.^{25,26} IP of Beclin1 could also pull down Bcl-xL but not Mcl-1

(Figure 4 and data not shown). Treatment with 10 μM (-)-gossypol abolished this Bcl-2–Beclin1 interaction, as indicated by the disappearance of the specific pull-down bands (Figure 4). (-)-Gossypol also abrogated the binding of Bcl-xL with Beclin1 (Figure 4). It has been shown that Beclin1 can be cleaved by the activated caspase-3.²⁷ Interestingly, Beclin1 cleavage was evident in WCLs and in ER-enriched fraction, but not in mitochondria, after treatment with (-)-gossypol (Figure 4). These data suggest a multifaceted BH3-mimetic capacity for (-)-gossypol, as an earlier report⁶ showed that (-)-gossypol was a potent inhibitor of pro-apoptotic proteins binding to the BH3-binding groove in Bcl-2/Bcl-xL. Our data show for the first time that (-)-gossypol can also interrupt the interactions between

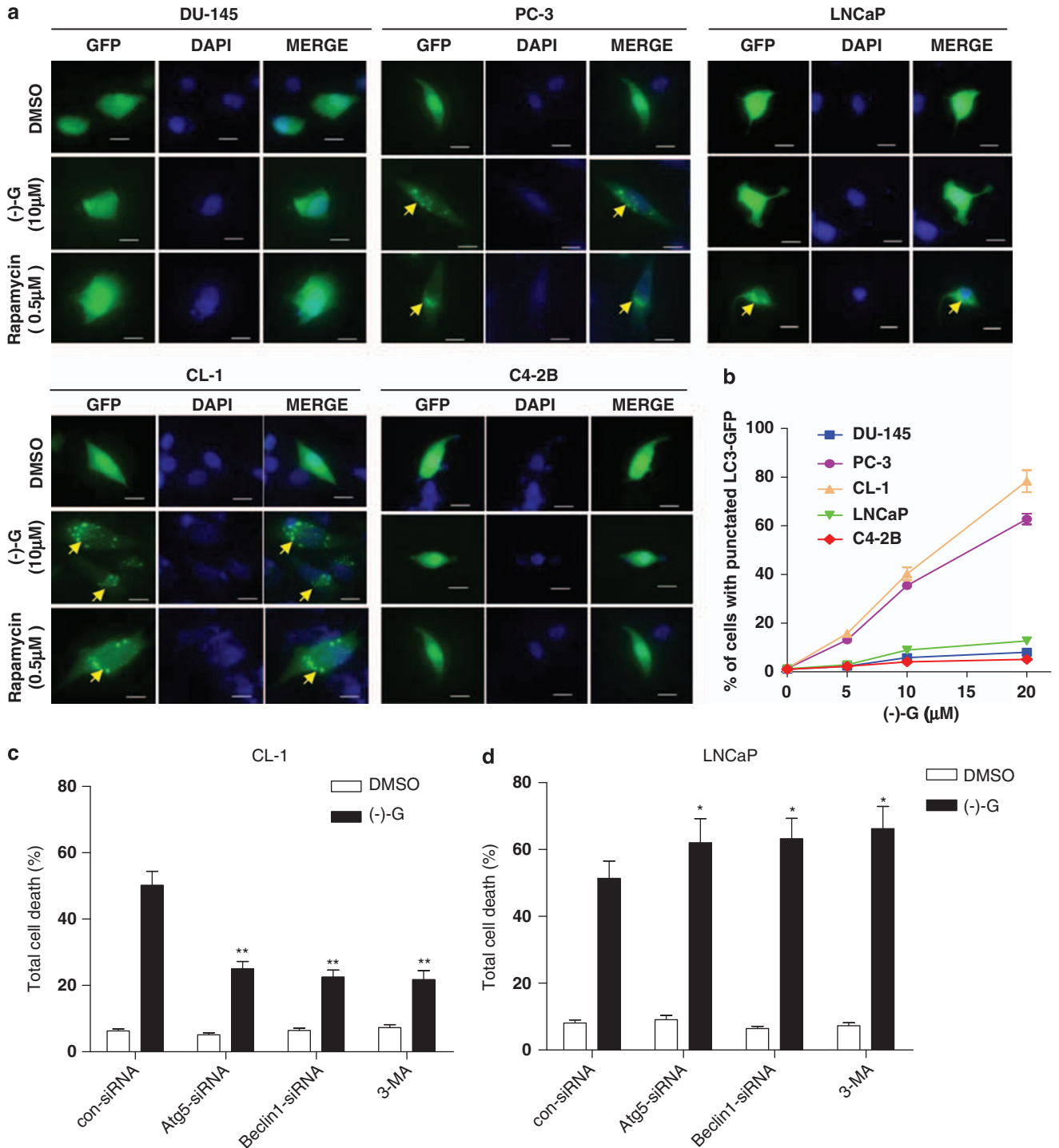


Figure 3 (-)-Gossypol preferentially induces autophagy in apoptosis-resistant prostate cancer cells as revealed by LC3-GFP puncta formation. **(a)** (-)-Gossypol-induced autophagy in prostate cancer cells as analyzed by LC3-GFP. Cells were transfected with LC3-GFP plasmid, treated with DMSO or 10 μM (-)-gossypol for 24 h, and then analyzed under a fluorescent microscope. The yellow arrows indicate the punctate pattern of LC3-GFP in autophagic cells. Treatment with 0.5 μM rapamycin was used as a positive control for autophagy induction. **(b)** Quantification of data from **(a)**, expressed as percentage of cells with punctate LC3-GFP (50 green fluorescent cells in one field, $n = 5$). **(c, d)** Effects of Atg5 or Beclin1 downregulation or 3-MA on the (-)-gossypol-induced cell death in CL-1 **(c)** and LNCaP cells **(d)**. Cells were transiently transfected either with a control siRNA or siRNA specific to Atg5 or Beclin1 or pre-treated with 5 mM 3-MA, and then treated with DMSO or (-)-gossypol for 24 h. Viability was assessed by Trypan blue staining. Results are means \pm S.D. of three independent experiments. ** $P < 0.01$ or * $P < 0.05$ by two-way ANOVA compared to (-)-G treatment of con-siRNA cells where indicated in panel **(c)** and **(d)**, respectively

Beclin1 and Bcl-2/Bcl-xL at ER, thus releasing the BH3-only pro-autophagic protein Beclin1, which in turn triggers the autophagic cascade.

To further delineate the role of Beclin1-Bcl-2 interaction in (-)-gossypol-induced autophagy, we modulated their intracellular protein levels by either siRNA knockdown or

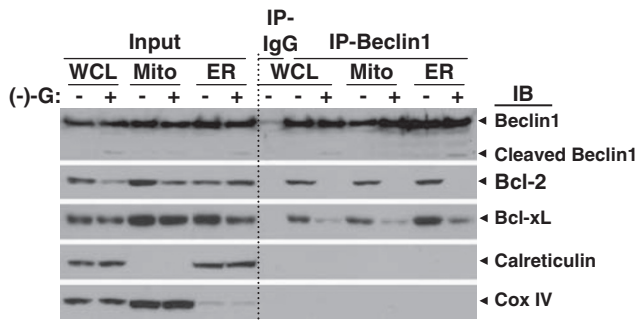


Figure 4 (–)-Gossypol modulates Bcl-2–Beclin1 interaction at the ER. Co-immunoprecipitation (co-IP) pull-down assay shows that (–)-gossypol specifically disrupts Bcl-2–Beclin1 interaction. CL-1 cells were treated with DMSO or 10 μ M (–)-gossypol for 6 h at 37°C and subjected to subcellular fractionation and IP with the indicated antibodies

exogenous overexpression in independent experiments. We used plasmid-encoded shRNA or siRNAs to knockdown Bcl-2 or Beclin expression, respectively, in PC-3 and CL-1 cells. The relative amount of LC3-II induced by (–)-gossypol increased upon Bcl-2 knockdown and decreased upon Bcl-2 overexpression in PC-3 and CL-1 cells (Figures 5a and c). (–)-Gossypol -induced total cell death increased when Bcl-2 was knocked down and decreased when it was exogenously overexpressed (Figures 5b and d). In contrast, Beclin1 knockdown by siRNA resulted in a decrease in (–)-gossypol-induced LC3-II and the latter was increased when Beclin1 was overexpressed (Figures 5e and f). Interestingly, overexpression of Bcl-2 in DU-145 cells that lack Bcl-2 did not increase the LC3-II (data not shown). These results show that the interaction and balance of Bcl-2 and Beclin1 have a key role in triggering autophagy by (–)-gossypol. More specifically, (–)-gossypol induces autophagy through modulating the interaction of Bcl-2 and Beclin1 and this process was further enhanced by either exogenously expressing Beclin1 or knocking down Bcl-2 protein levels in cells with high Bcl-2.

(–)-Gossypol regulates autophagy pathway-associated genes in prostate cancer cells. To investigate the effects of (–)-gossypol on genes associated with the autophagy pathway, we carried out Human Autophagy PCR Array analysis in CL-1 cells treated with either DMSO or 10 μ M (–)-gossypol. As shown in Figure 6a, 10 μ M (–)-gossypol treatment for 24 h upregulated autophagy-associated genes including *atg12*, *atg5*, *becn1* (the gene for Beclin1), *map1lc3b*, and *vps34*. On the other hand, certain anti-autophagic genes were downregulated, namely *akt1s1* and *bcl2* (for full array data set, see Supplementary Table 1). Figure 6b shows the qRT-PCR validation of Bcl-2 and Beclin1 expression, which again demonstrates that (–)-gossypol upregulates Beclin1 and downregulates Bcl-2 mRNA levels. Finally, immunoblotting showed that (–)-gossypol indeed increased protein levels of Beclin1, Atg5-Atg12, Vps34, and LC3-II when compared with DMSO control, but reduced the relative amount of Bcl-2 (Figure 6c), whereas no effect on the expression levels of Bcl-xL and Mcl-1 was observed (Supplementary Figure S6). Our data show that (–)-gossypol upregulates the genes

involved in the autophagy process and downregulates Bcl-2, which is an important anti-autophagy gene.

To determine whether (–)-gossypol affects Beclin1 upregulation and Bcl-2 downregulation at the level of transcription, translation, or both, we blocked protein synthesis with cycloheximide (CHX) and assessed relevant protein levels in CL-1 cells with or without (–)-gossypol treatment. In a time course experiment, (–)-gossypol increased Beclin1 protein levels at all time points tested with an apparent peak at 24 h. This is correlated with the time course of (–)-gossypol-induced autophagy shown in Figure 1c. (–)-Gossypol also accelerated the degradation of Beclin1 after protein synthesis was inhibited, with the Beclin1 protein half-life reduced from 61 h (CHX) to 42 h (CHX + G) (Supplementary Figure 7A). On one hand, (–)-gossypol reduced Bcl-2 protein level at 16 h with a half-life ($T_{1/2}$) of 60 h, and on the other, it decreased the degradation of Bcl-2 after protein synthesis was inhibited, with the protein half-life increased from 31 h (CHX) to 36 h (CHX + G) (Supplementary Figure 7B). Together with qRT-PCR data, these results suggest that the transcriptional effects of (–)-gossypol treatment (increased Beclin1 and decreased Bcl-2) most likely overshadow any post-translational affect on their protein levels.

Atg5 is required for (–)-gossypol-induced autophagy.

It has been reported that Atg5 is required for formation of autophagosomes, and Atg5-deficient mouse embryonic stem cells show significantly diminished numbers of autophagic vesicles.²⁸ Immunoblotting showed a 60–80% reduction of Atg5–Atg12 in CL-1 and PC-3 cells transiently transfected with a pool of three Atg5-targeted siRNAs, confirming knockdown of this protein (Figure 6d). Knocking down Atg5 in CL-1 and PC-3 cells suppressed the conversion of LC3-I to LC3-II that normally ensues after a 24-h exposure to (–)-gossypol (Figure 6d), whereas little effect was observed in nonspecific siRNA-transfected cells. In addition, (–)-gossypol treatment (10 μ M, 24 h) of control siRNA-transfected cells caused a significant increase in the fraction of cells with punctate LC3 over DMSO-treated control. No significant puncta were observed in cells transfected with Atg5-siRNA and treated with (–)-gossypol (Figure 6e). Together, these results indicate that Atg5 is required for the (–)-gossypol-induced autophagy.

(–)-Gossypol inhibited CL-1 and PC-3 xenograft tumor growth *in vivo* in association with increased autophagy in the tumors.

We carried out animal experiments to examine whether (–)-gossypol induces autophagy *in vivo*. As shown in Figure 7a, oral administration of (–)-gossypol daily at 20 mg/kg dose significantly inhibited xenograft growth ($P < 0.001$ versus vehicle control, $n = 10$). The animal body weights of the control and (–)-gossypol-treated mice did not differ significantly throughout the experimental protocol (data not shown). A vast majority of the tumor cells (~80%) from the (–)-gossypol treatment group showed obvious membranous vacuoles resembling autophagosomes compared with an insignificant percentage of control tumor cells (Figure 7b). During the treatment course, tumors from (–)-gossypol-treated mice showed increased LC3-II conversion together with increased Beclin1 and decreased

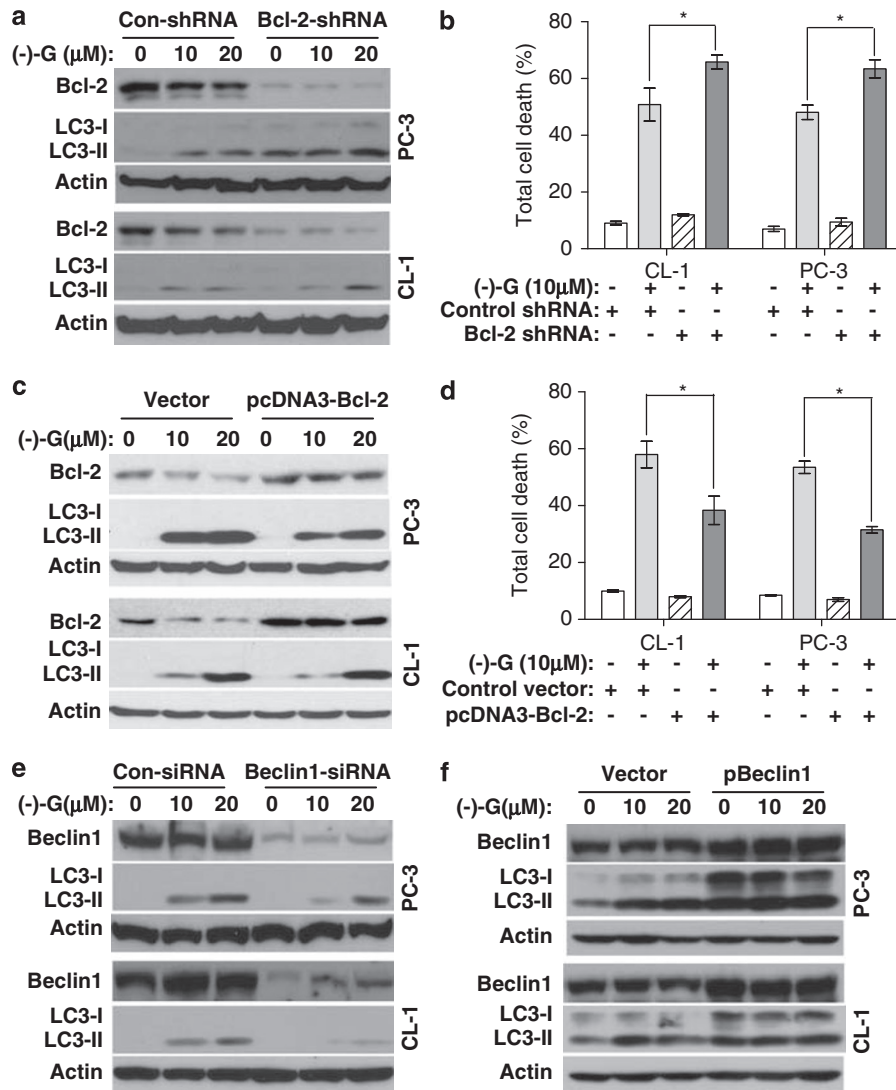


Figure 5 Effects of modulating Bcl-2 or Beclin1 protein levels on (–)-gossypol-induced autophagy and cell death in PC-3 and CL-1 cells. (a–f) Cells were transiently transfected with either control shRNA/siRNA or shRNA/siRNA specific to Bcl-2 (a)/Beclin1 (e), or expression vectors for Bcl-2 (b) or Beclin1 (f). At 24 h after transfection, cells were treated with DMSO or (–)-gossypol for 24 h, and then subjected to either immunoblot analysis for Bcl-2, Beclin1, and LC3 or Trypan blue staining (b, d). * $P < 0.05$ between the indicated groups by two-way ANOVA in panels (b) and (d)

Bcl-2 protein levels (Figure 7c, Supplementary Figure 8). Human Autophagy PCR Array analysis of the tumors (Figure 7d) showed upregulation of the autophagy-associated genes, including *atg5*, *atg12*, *becn1*, *map1lc3b*, *vps34*, and so on, and downregulation of *bcl2*, analogous to our *in vitro* data. Similar results were observed in another AI tumor model, the PC-3 xenograft model in nude mice, in which orally active (–)-gossypol also induced autophagy *in vivo* (Figures 7e and f). These results show that (–)-gossypol potentially inhibited the growth of AI prostate tumor with high levels of Bcl-2, accompanied by autophagy induction *in vivo*.

Discussion

In this study, we investigated the mechanisms of cell death induced by (–)-gossypol, a natural BH3-mimetic small-molecule inhibitor of Bcl-2, in human prostate cancer. Our *in vitro* and *in vivo* studies show that (–)-gossypol

preferentially induces autophagic cell death in apoptosis-resistant AI prostate cancer CL-1 and PC-3 cells with high levels of Bcl-2/xL but not in apoptosis-sensitive cells with low Bcl-2/xL. Meanwhile, (–)-gossypol preferentially induces apoptosis in human prostate cancer LNCaP (AD with low levels of Bcl-2/xL), DU-145, and C4-2B cells (AI but lacking Bcl-2). (–)-Gossypol potentially blocks the Bcl-2–Beclin1 interaction at ER, downregulates Bcl-2, and upregulates Beclin1. (–)-Gossypol-induced autophagic cell death is Atg5 dependent, and can be attenuated by Bcl-2 overexpression and enhanced by Beclin1 overexpression. Treatment with (–)-gossypol also upregulated the expression of autophagy-related genes in CL-1 and PC-3 cells both *in vitro* and *in vivo*. Taken together, our data show that this pan-Bcl-2 inhibitor exerts its antitumor activity by preferentially inducing autophagy in the apoptosis-resistant, AI prostate cancer cells with high levels of Bcl-2, through modulation of Bcl-2–Beclin1 interactions at the ER.

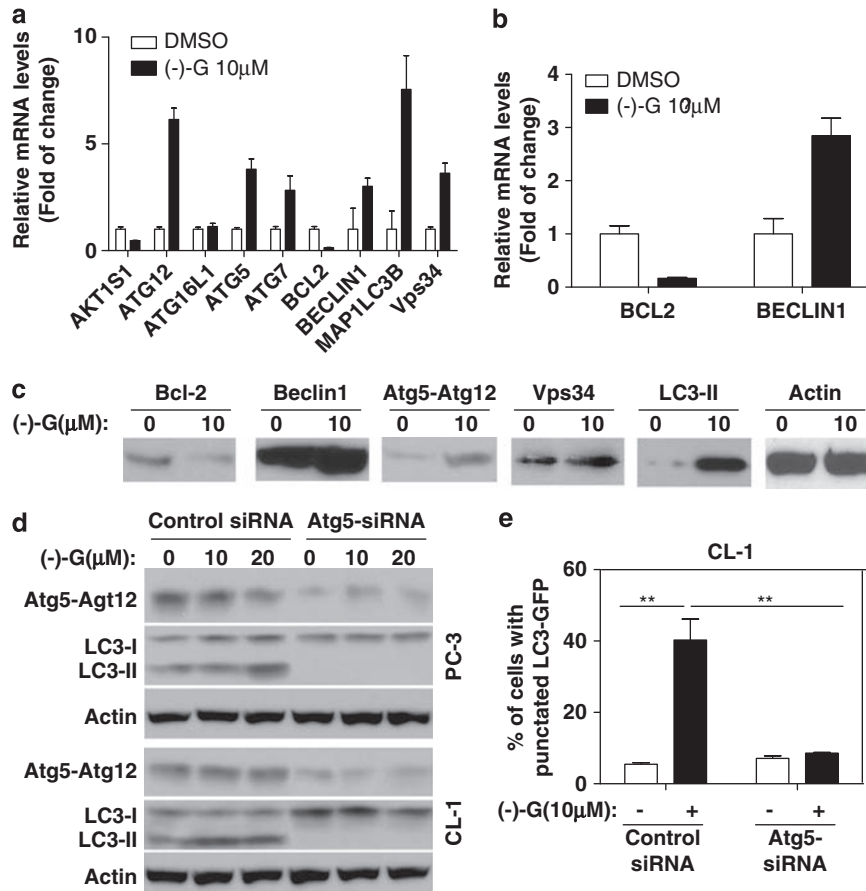


Figure 6 (-)-Gossypol regulates autophagy pathway-associated genes in prostate cancer cells. (a) Human Autophagy PCR Array analysis of the autophagy-associated gene expression levels in CL-1 cells treated with DMSO or 10 μ M (-)-gossypol. ($n = 2$). (b) qRT-PCR validation of Bcl-2 and Beclin1 expression. (c) Western blot confirmation of the protein-level changes of the most regulated genes identified by PCR Array. (d) PC-3 and CL-1 cells were transiently transfected with either control siRNA or SmartPool Atg5-siRNAs for 24 h, and then treated with DMSO or (-)-gossypol for 24 h. The cells were lysed for immunoblot analysis of Atg5-12 and LC3. (e) Percentage of cells with punctate GFP-LC3 in CL-1 cells transiently transfected with control siRNA or Atg5-siRNA treated with DMSO (control) or 10 μ M (-)-gossypol for 24 h. $**P < 0.01$ between the indicated groups by two-way ANOVA

Targeting the autophagic pathway to kill cancer cells has emerged as a promising new avenue for drug discovery and cancer therapy. Although BH3 mimetics were originally designed to stimulate apoptosis, their potential as inducers of autophagy has recently come to light. For example, ABT-737 has been shown to inhibit the interaction of Bcl-2 and Bcl-xL with pro-apoptotic proteins as well as the pro-autophagic protein Beclin-1.^{29,30} The ability of ABT-737 to stimulate apoptosis has been associated with high levels of Bcl-2 in lymphoma and has been extensively studied in many other cancer cell types.³¹ Concomitant stimulation of apoptosis and autophagy with BH3-mimetic ABT-737 and rapamycin, respectively, along with IR gave promising results in a lung cancer model.³² Our study shows for the first time that BH3-mimetic (-)-gossypol can induce autophagy *versus* apoptosis depending on cellular context, and we have associated different modes of cell death with low Bcl-2 AD prostate cancer cells or high Bcl-2 AI ones. On the basis of our data, we propose a working model, as illustrated in Figure 8, on the potential molecular mechanism of action of (-)-gossypol-induced autophagic cell death in AI prostate cancer cells with high Bcl-2.

Bcl-xL and Bcl-2 are anti-apoptotic and anti-autophagic proteins, mainly residing on the mitochondrial and ER membranes. Under normal growth conditions, they repress the induction of both apoptosis and autophagy.³³ As illustrated in our working model (Figure 8), (-)-gossypol-induced mode of cell death is cellular context dependent. When the expression levels of Bcl-2/xL are low, such as in LNCaP, DU-145, and C4-2B cells, (-)-gossypol preferentially induces apoptosis. On the other hand, when Bcl-2 is highly expressed, such as in AI prostate cancer PC-3 and CL-1 cells, (-)-gossypol preferentially induces autophagy. Bcl-2 and Bcl-xL bind to Bad, Bak, or Bax on mitochondria. When cells are exposed to (-)-gossypol, it binds to Bcl-2/Bcl-xL, thus liberating Bax and/or Bak to homo-oligomerize and trigger apoptosis.³⁴ In AI prostate cancer cells that are resistant to apoptosis because of high levels of Bcl-2, the overexpressed Bcl-2 binds to Beclin1 at ER, and sequesters Beclin1 from inducing autophagy. In this study we uncover a novel function for (-)-gossypol as a BH3-mimetic inhibitor. By blocking the BH3-domain-dependent interaction between Bcl-2/Bcl-xL and Beclin1, Atg5- and Beclin1-dependent autophagy ensues. Further study is required to determine

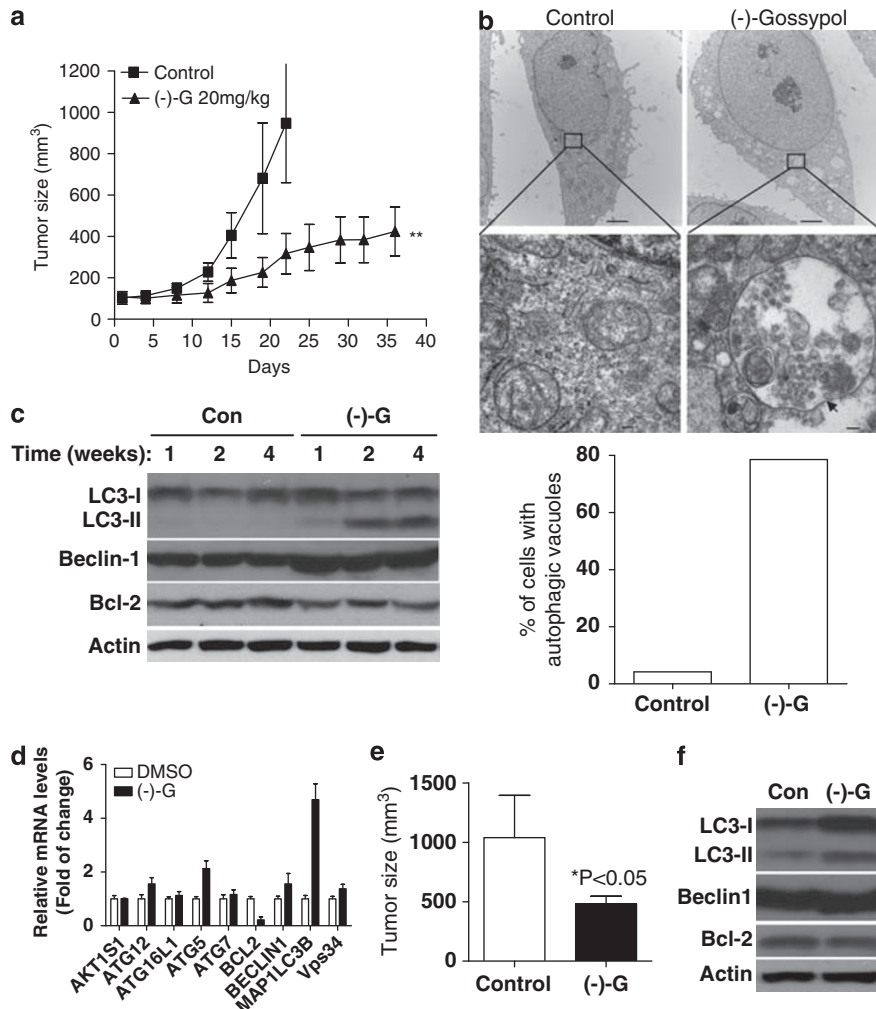


Figure 7 Oral administration of (–)-gossypol inhibited CL-1 and PC-3 xenograft growth and was associated with increased LC3-II conversion in the tumors. (a) (–)-gossypol potently inhibited the CL-1 xenograft tumor growth in nude mice as a single-agent oral therapy. CL-1 cells (2×10^6) were s.c. injected into the flanks on both sides of each mouse. When the tumors reached 100 mm^3 , the mice were randomized into 5–8 mice per group. (–)-Gossypol was administered p.o. through oral gavage, daily at a 20 mg/kg dose. The data shown are average tumor size (means \pm S.E.M., $n = 10$). ** $P < 0.01$, versus vehicle control, two-way ANOVA ($n = 10$). (b) Representative electron micrograph image showing autophagic vacuoles with content after (–)-gossypol treatment in an *in vivo* CL-1 xenograft model. The percentage of cells with autophagic vacuoles was quantified in 50 cells per group. (c) (–)-Gossypol-induced autophagy in CL-1 xenograft tumors *in vivo*. CL-1 xenograft tumor tissue lysates from the vehicle control group or (–)-gossypol treatment group were immunoblotted for Beclin1, LC3, and Bcl-2 at the indicated time points. (d) Modulation of the autophagy-associated gene expression in tumor tissues after treatment with DMSO or (–)-gossypol for 2 weeks. Gene expression was detected using Human Autophagy PCR Array and the data are shown as relative mRNA levels ($n = 2$). (e) (–)-Gossypol potently inhibited the PC-3 xenograft tumor growth in nude mice as a single-agent oral therapy. Study was conducted as in (a) and tumor size data were collected at 5 weeks. (f) (–)-Gossypol-induced autophagy *in vivo* in PC-3 xenograft model in nude mice. Immunoblotting for Beclin1, LC3, and Bcl-2 using lysates from PC-3 xenograft tumor tissues treated with vehicle or (–)-gossypol for 3 weeks. * $P < 0.05$ by two-way ANOVA

why (–)-gossypol induces autophagy when Bcl-2 levels are superphysiological compared with normal prostate epithelium. Regardless of this, the finding that inhibition of Bcl-2/Bcl-xL binding to Beclin1 at the ER by BH3 mimetics, including (–)-gossypol, can stimulate autophagic cell death in certain situations will undoubtedly influence Bcl-2 drug design/discovery and the mechanistic study of cancer cell death.

The connection between apoptotic (type I cell death) and autophagic cell death (type II cell death) in the context of cancer-relevant stimuli is still unresolved, but a compensatory relationship may exist. For example, inhibition of autophagy by chloroquine has been shown to increase vorinostat-mediated apoptosis in colon cancer cells.³⁵ Furthermore, the autophagy inhibitors 3-MA and chloroquine

have been shown to synergistically augment the pro-apoptotic response to a histone deacetylase inhibitor.³⁶ Conversely, inhibiting the activity of caspase-3 enhanced autophagic cell death in lung cancer cells.³⁷ The results of the present study are unique in that either apoptosis or autophagy can be induced by BH3-mimetic (–)-gossypol in prostate cancer cells, depending on cellular context, that is, AD and Bcl-2 levels. In cells with low Bcl-2, decreasing Bcl-2 levels along with inhibiting the interaction of Bcl-2 with pro-apoptotic BH3-containing proteins may be enough to tip the scale toward apoptosis. On the other hand, in cells with excess Bcl-2, perhaps the induction of autophagy occurs more quickly when Beclin1 binding to Bcl-2/xL is blocked by the BH3-mimetic (–)-gossypol. Beclin1 localizes mainly

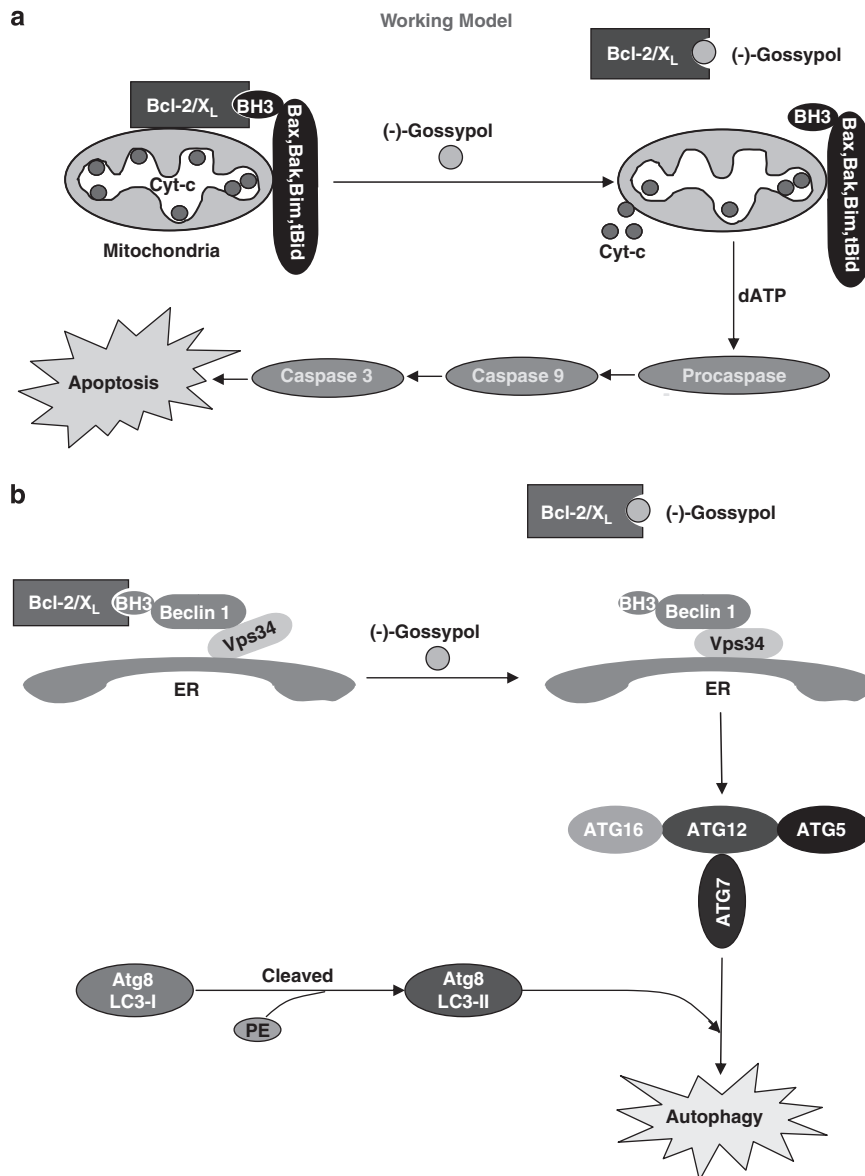


Figure 8 Model for the mechanisms of action of (-)-gossypol, indicating that the mode of cell death induced by (-)-gossypol is cellular context dependent. **(a)** In androgen-dependent (AD) prostate cancer cells that have low levels of Bcl-2/xL and are sensitive to apoptosis, for example, LNCaP, (-)-gossypol potentially binds to Bcl-2/xL at mitochondria, releasing Bax/Bak and inducing apoptotic cell death. **(b)** In androgen-independent (AI) prostate cancer cells that have high levels of Bcl-2/xL and are resistant to apoptosis, for example, CL-1 and PC-3, (-)-gossypol potentially binds to Bcl-2/xL and releases Beclin1 at ER, and thus preferentially induces autophagic cell death

at ER,^{21,22} in which it is sequestered by excessive Bcl-2, and we have shown that Beclin-1 is intrinsic to autophagy induction by (-)-gossypol. In this study we show for the first time that, in AI prostate cancer cells with high Bcl-2, (-)-gossypol can indeed act at the ER to block the Beclin1–Bcl-2 interaction. As autophagy induction is thought to occur mostly at the ER, the fact that (-)-gossypol acts on mitochondria-associated Beclin1 seems most likely inconsequential. Previous reports on ABT-737 have shown that in certain contexts it can affect Beclin1–Bcl-2/xL interactions specifically at the ER.^{21,22} This difference highlights the fact that in addition to Bcl-2 family member binding specificity (pan *versus* Bcl-2/xL specific), not all Bcl-2 inhibitors have the same subcellular mechanisms of action.

In conclusion, our study shows that the BH3-mimetic (-)-gossypol potentially induces autophagic cell death in human AI prostate cancer with a high level of Bcl-2 both *in vitro* and *in vivo*. This may represent a novel molecular mechanism for the treatment of hormone-refractory prostate cancer with Bcl-2 overexpression. In fact, based on the positive results from Phase II trials in patients with castration-resistant prostate cancer, (-)-gossypol is now in Phase IIb clinical trials for advanced prostate cancer. Our results provide new insights into how (-)-gossypol can induce cell death by different mechanisms, and highlight the importance of the interplay between apoptosis and autophagy. Defining the molecular profile of tumors in each cancer patient and exploiting the potential of autophagy to kill cancer cells may

lead to rationally designed molecularly targeted therapies that ultimately improve patient outcomes.

Materials and Methods

Cell culture and reagents. Cell culture reagents and fetal bovine serum (FBS) were purchased from HyClone (Waltham, MA, USA). Human prostate cancer cell lines were obtained from American Type Culture Collection except the LNCaP-derived sublines CL-1 and C4-2B. All prostate cancer cell line CL-1 was derived from its parental AD cells LNCaP and was provided by Dr. Arie Belldegrun at the University of California–Los Angeles.³⁸ C4-2B cell line was provided by Dr. Kenneth Pienta at the University of Michigan and maintained in T-medium supplemented with 10% (v/v) FBS and antibiotics. LNCaP, CL-1, PC-3, and DU-145 cells were cultured in DMEM nutrient mixture supplemented with 10% FBS and antibiotics. Normal human prostate epithelial cell line (PrEC) was purchased from Clonetics (Walkersville, MD, USA) and maintained in PrEBM (Cambrex). (–)-Gossypol was purified from natural racemic gossypol as we previously described,^{14,39} and dissolved in DMSO at 20 mM as stock solution. 3-MA, rapamycin, and acridine orange were from Sigma-Aldrich (Louis, MO, USA); caspase-3/CPP32 fluorometric assay kit was from Biovision (Mountain view, CA, USA); antibodies against microtubule-associated protein 1 light chain 3 (LC3), PARP, Atg5, Atg10, and Bcl-xL were from Cell Signaling (Boston, MA, USA); and the antibodies against Bcl-2, Mcl-1, and Beclin1 were from Santa Cruz (Santa Cruz, CA, USA). The antibody against PIK3C3 was from AbCam (Cambridge, MA, USA). LC-3 cDNA was kindly provided by Drs. N Mizushima and T Yoshimori at Osaka University, Japan. Beclin1 and Bcl-2 expression vectors were purchased from OriGene (Rockville, MD, USA).

GFP-LC3 analysis. Cells were transfected with GFP-LC3 vector using Lipofectamine 2000 (Invitrogen Life Technologies, Carlsbad, CA, USA). After 24 h, cells were treated with DMSO (control), (–)-gossypol (10 μ M), or rapamycin (0.5 μ M) for 24 h, and then fixed in 4% formaldehyde for 10 min. Cells were then washed thrice with PBS and stained with DAPI, and observed under a fluorescence microscope (OLYMPUS IX71, Center Valley, PA, USA) with $\times 60$ lens.

Transmission electron microscopy (TEM). Cells (1×10^6) were seeded in 10 cm dishes and allowed to attach overnight. The cells were treated with either DMSO (final concentration, < 0.1%) or 10 μ mol/l (–)-gossypol for 24 h at 37°C. Cells were fixed in ice-cold 2.5% electron microscopy grade glutaraldehyde (in 0.1 mol/l PBS (pH 7.3)), rinsed with PBS, postfixed in 1% osmium tetroxide with 0.1% potassium ferricyanide, dehydrated through a graded series of ethanol (30–90%), and embedded in Epon. Semithin sections (300 nm) were cut using a Reichart Ultracut (Leica Microsystems Inc., Chicago, IL, USA), stained with 0.5% toluidine blue, and examined under a light microscope. Ultrathin sections (65 nm) were stained with 2% uranyl acetate and Reynold's lead citrate and examined using JEOL 1210 transmission electron microscope (Tokyo, Japan).

Subcellular fractionation and co-IP experiments. CL-1 cells (5×10^6) were plated on 15 cm dishes and allowed to attach overnight. After treatment with either DMSO or 10 μ M (–)-gossypol for 6 h at 37°C, the mitochondria fractions and enriched ER fractions were separated by differential centrifugation after hypotonic lysis and dounce homogenization in 20 mM Hepes-KOH pH 7.5, 10 mM KCl, 1.5 mM MgCl₂, 1 mM sodium EDTA, 1 mM sodium EGTA, 1 mM DTT, and 250 mM sucrose + complete cocktail protease inhibitors. WCL was generated by collecting the supernatant of a low speed spin (1000 $\times g$) to pellet nuclei. The mitochondrial pellet was resuspended in the same hypotonic lysis buffer and all fractions were supplement with CHAPS to a final concentration of 2%. WCL and fractions were pre-cleared with protein A-agarose, and then mixed with Beclin1 antibodies or control IgG for 1 h at 4°C (each IP reaction consisted of 1 mg total protein). The immunoprecipitates were captured on protein A-agarose and analyzed by immunoblotting with antibodies against Beclin1, Bcl-2, or Bcl-xL, respectively.

PCR array and qRT-PCR. Total RNA was extracted from the treated cells using TRIzol (Invitrogen, Carlsbad, CA, USA). Reverse transcription was performed using Super-Script III First-Strand kits (Invitrogen). For PCR array, we used human autophagy primer library (HATPL-1) from RealTime Primers LLC (Elkins Park, PA, USA) and SYBR green PCR master mix (Applied Biosystems, Foster city, CA, USA), according to the manufacturer's instruction. The PCR array data were validated by qRT-PCR using TaqMan Universal PCR Master Mix

(Applied Biosystems; 95°C for 10 min, 40 cycles of 95°C for 15 s, and 60°C for 1 min).⁴⁰ Primers were designed as Beclin1 forward 5'-CAAGATCCTGGAC CGTGTC-3' and reverse 5'-TGGCACTTTCTGTGGACATCA-3', Bcl-2 forward 5'-TGCACCTGACGCCCTTAC-3' and reverse 5'-AGACAGCCAGGAGAAATCAA CAG-3', and β -actin forward 5'-GCCAACACAGTGTCTGTGG-3' and reverse 5'-GCTCAGGAGGAGCAATGATCTTG-3'.

Small interfering RNA transfection. siRNAs to Beclin1, Bcl-2, Atg5, or control siRNA were obtained from Dharmacon (Lafayette, CO, USA). Cells were plated in six-well plates and transfected with siRNA (100 pmol/well) by Lipofectamine 2000 according to the manufacturer's manual. (–)-Gossypol was added to the cells 24 h after transfection. For western blot, cells were collected after an additional 24 h culture.

Animal studies. *In vivo* experiments were carried out with 5- to 6-week-old female NCr-nu/nu nude mice purchased from the National Cancer Institute (Bethesda, MD, USA). Mice were inoculated s.c. with 0.2 ml CL-1 cell suspension (2×10^6 cells) using a sterile 22-gauge needle. When tumors reached 100 mm³, the mice were randomized into two groups with 5–8 mice per group. Group 1 was given carboxymethyl cellulose (CMC) as vehicle control; group 2 was given (–)-gossypol in CMC, 20 mg/kg, p.o. daily for 3 weeks. The tumor sizes and animal body weights were measured twice weekly and plotted as we previously described.¹⁴ At 1, 2, and 3 weeks, one mouse from each group was killed and the tumors were dissected. Tumor tissues were processed for western blot.¹⁴ All animal experiments were carried out according to the protocol approved by the University of Michigan Guidelines for Use and Care of Animals.

Statistical analysis. Two-tailed Student's *t*-test and two-way ANOVA were used to analyze the *in vitro* and *in vivo* data, respectively, using Prism 5.0 software (GraphPad Prism, San Diego, CA, USA). A threshold of $P < 0.05$ was defined as statistically significant.

Conflict of interest

Dr Xu is a co-inventor of a patent related to this study; he is funded by NIH and receives no funding from industry. All other authors declare no competing interest.

Acknowledgements. This study was supported in part by NIH grants CA121830(S1), CA128220, and CA134655 (to LX), and by NIH through the University of Michigan's Cancer Center Support Grant (P30 CA46592). We thank Drs. N Mizushima and T Yoshimori at Osaka University, Japan, for kindly providing LC3 cDNA; Dr. Arie Belldegrun at University of California–Los Angeles for kindly providing CL-1 cells; Dr. Kenneth Pienta at University of Michigan for kindly providing C4-2B cells; Dr. Dorothy Sorenson in the University of Michigan Comprehensive Cancer Center (UMCCC) Microscopy and Image Analysis Laboratory for help with TEM analysis; UMCCC Flow Cytometry Core for flow cytometry analysis; Histology Core for the immunohistology study; and the Unit of Laboratory Animal Medicine (ULAM) for help with animal experiments.

- Assikis VJ, Simons JW. Novel therapeutic strategies for androgen-independent prostate cancer: an update. *Semin Oncol* 2004; **31** (2 Suppl 4): 26–32.
- Oh WK, Kantoff PW. Management of hormone refractory prostate cancer: current standards and future prospects.[see comment]. [Review] [107 refs]. *J Urol* 1998; **160**: 1220–1229.
- Rago R. Management of hormone-sensitive and hormone-refractory metastatic prostate cancer. *Cancer Control* 1998; **5**: 513–521.
- Martin AP, Park MA, Mitchell C, Walker T, Rahmani M, Thorburn A *et al*. BCL-2 family inhibitors enhance histone deacetylase inhibitor and sorafenib lethality via autophagy and overcome blockade of the extrinsic pathway to facilitate killing. *Mol Pharmacol* 2009; **76**: 327–341.
- Lin J, Zheng Z, Li Y, Yu W, Zhong W, Tian S *et al*. A novel Bcl-XL inhibitor Z36 that induces autophagic cell death in HeLa cells. *Autophagy* 2009; **5**: 314–320.
- Kitada S, Leone M, Sareth S, Zhai D, Reed JC, Pellecchia M. Discovery, characterization, and structure-activity relationships studies of proapoptotic polyphenols targeting B-cell lymphocyte/leukemia-2 proteins. *J Med Chem* 2003; **46**: 4259–4264.
- Extebarria A, Landeta O, Antonsson B, Basanez G. Regulation of antiapoptotic MCL-1 function by gossypol: mechanistic insights from *in vitro* reconstituted systems. *Biochem Pharmacol* 2008; **76**: 1563–1576.

8. Liu S, Kulp SK, Sugimoto Y, Jiang J, Chang HL, Dowd MK *et al*. The (–)-enantiomer of gossypol possesses higher anticancer potency than racemic gossypol in human breast cancer. *Anticancer Res* 2002; **22** (1A): 33–38.
9. Oliver CL, Bauer JA, Wolter KG, Ubell ML, Narayan A, O'Connell KM *et al*. *In vitro* effects of the BH3 mimetic, (–)-gossypol, on head and neck squamous cell carcinoma cells. *Clin Cancer Res* 2004; **10**: 7757–7763.
10. Loberg RD, McGregor N, Ying C, Sargent E, Pienta KJ. *In vivo* evaluation of AT-101 (R(–)-gossypol acetic acid) in androgen-independent growth of VCaP prostate cancer cells in combination with surgical castration. *Neoplasia* 2007; **9**: 1030–1037.
11. Priyadarshi A, Roy A, Kim KS, Kim EE, Hwang KY. Structural insights into mouse anti-apoptotic Bcl-xl reveal affinity for Beclin 1 and gossypol. *Biochem Biophys Res Commun* 2010; **394**: 515–521.
12. Patel MP, Masood A, Patel PS, Chanan-Khan AA. Targeting the Bcl-2. *Curr Opin Oncol* 2009; **21**: 516–523.
13. Xu L, Yang D, Wang S, Tang W, Liu M, Davis M *et al*. Gossypol enhances response to radiation therapy and results in tumor regression of human prostate cancer. *Mol Cancer Ther* 2005; **4**: 197–205.
14. Meng Y, Tang W, Dai Y, Wu X, Liu M, Ji Q *et al*. Natural BH3 mimetic (–)-gossypol chemosensitizes human prostate cancer via Bcl-xL inhibition accompanied by increase of Puma and Noxa. *Mol Cancer Ther* 2008; **7**: 2192–2202.
15. Hoyer-Hansen M, Jaattela M. Autophagy: an emerging target for cancer therapy. *Autophagy* 2008; **4**: 574–580.
16. Cuervo AM. Autophagy: many paths to the same end. *Mol Cell Biochem* 2004; **263**: 55–72.
17. Shintani T, Klionsky DJ. Autophagy in health and disease: a double-edged sword. *Science* 2004; **306**: 990–995.
18. Kondo Y, Kanzawa T, Sawaya R, Kondo S. The role of autophagy in cancer development and response to therapy. *Nat Rev Cancer* 2005; **5**: 726–734.
19. Bursch W, Ellinger A, Kienzl H, Torok L, Pandey S, Sikorska M *et al*. Active cell death induced by the anti-estrogens tamoxifen and ICI 164 384 in human mammary carcinoma cells (MCF-7) in culture: the role of autophagy. *Carcinogenesis* 1996; **17**: 1595–1607.
20. Levine B, Sinha S, Kroemer G. Bcl-2 family members: dual regulators of apoptosis and autophagy. *Autophagy* 2008; **4**: 600–606.
21. Maiuri MC, Ciriollo A, Tasdemir E, Vicencio JM, Tajeddine N, Hickman JA *et al*. BH3-only proteins and BH3 mimetics induce autophagy by competitively disrupting the interaction between Beclin 1 and Bcl-2/Bcl-X(L). *Autophagy* 2007; **3**: 374–376.
22. Wang J. Beclin 1 bridges autophagy, apoptosis and differentiation. *Autophagy* 2008; **4**: 947–948.
23. Paglin S, Hollister T, Delohery T, Hackett N, McMahon M, Sphicas E *et al*. A novel response of cancer cells to radiation involves autophagy and formation of acidic vesicles. *Cancer Res* 2001; **61**: 439–444.
24. Iwamaru A, Kondo Y, Iwado E, Aoki H, Fujiwara K, Yokoyama T *et al*. Silencing mammalian target of rapamycin signaling by small interfering RNA enhances rapamycin-induced autophagy in malignant glioma cells. *Oncogene* 2007; **26**: 1840–1851.
25. Sinha S, Levine B. The autophagy effector Beclin 1: a novel BH3-only protein. *Oncogene* 2008; **27** (Suppl 1): S137–S148.
26. Sinha S, Colbert CL, Becker N, Wei Y, Levine B. Molecular basis of the regulation of Beclin 1-dependent autophagy by the gamma-herpesvirus 68 Bcl-2 homolog M11. *Autophagy* 2008; **4**: 989–997.
27. Luo S, Rubinsztein DC. Apoptosis blocks Beclin 1-dependent autophagosome synthesis: an effect rescued by Bcl-xL. *Cell Death Differ* 2010; **17**: 268–277.
28. Pyo JO, Nah J, Kim HJ, Lee HJ, Heo J, Lee H *et al*. Compensatory activation of ERK1/2 in Atg5-deficient mouse embryo fibroblasts suppresses oxidative stress-induced cell death. *Autophagy* 2008; **4**: 315–321.
29. Kang MH, Reynolds CP. Bcl-2 inhibitors: targeting mitochondrial apoptotic pathways in cancer therapy. *Clin Cancer Res* 2009; **15**: 1126–1132.
30. Stauffer SR. Small molecule inhibition of the Bcl-X(L)-BH3 protein-protein interaction: proof-of-concept of an *in vivo* chemopotentiator ABT-737. *Curr Top Med Chem* 2007; **7**: 961–965.
31. Jayanthan A, Howard SC, Trippett T, Horton T, Whitlock JA, Daisley L *et al*. Targeting the Bcl-2 family of proteins in Hodgkin lymphoma: *in vitro* cytotoxicity, target modulation and drug combination studies of the Bcl-2 homology 3 mimetic ABT-737. *Leuk Lymphoma* 2009; **50**: 1174–1182.
32. Kim KW, Moretti L, Mitchell LR, Jung DK, Lu B. Combined Bcl-2/mammalian target of rapamycin inhibition leads to enhanced radiosensitization via induction of apoptosis and autophagy in non-small cell lung tumor xenograft model. *Clin Cancer Res* 2009; **15**: 6096–6105.
33. Levine B, Kroemer G. Autophagy in the pathogenesis of disease. *Cell* 2008; **132**: 27–42.
34. Paoluzzi L, Gonen M, Gardner JR, Mastrella J, Yang D, Holmlund J *et al*. Targeting Bcl-2 family members with the BH3 mimetic AT-101 markedly enhances the therapeutic effects of chemotherapeutic agents in *in vitro* and *in vivo* models of B-cell lymphoma. *Blood* 2008; **111**: 5350–5358.
35. Walker T, Mitchell C, Park MA, Yacoub A, Graf M, Rahmani M *et al*. Sorafenib and vorinostat kill colon cancer cells by CD95-dependent and -independent mechanisms. *Mol Pharmacol* 2009; **76**: 342–355.
36. Carew JS, Nawrocki ST, Kahue CN, Zhang H, Yang C, Chung L *et al*. Targeting autophagy augments the anticancer activity of the histone deacetylase inhibitor SAHA to overcome Bcr-Abl-mediated drug resistance. *Blood* 2007; **110**: 313–322.
37. Kim MS, Jeong EG, Ahn CH, Kim SS, Lee SH, Yoo NJ. Frameshift mutation of UVRAG, an autophagy-related gene, in gastric carcinomas with microsatellite instability. *Hum Pathol* 2008; **39**: 1059–1063.
38. Liu AY, Brubaker KD, Goo YA, Quinn JE, Kral S, Sorensen CM *et al*. Lineage relationship between LNCaP and LNCaP-derived prostate cancer cell lines. *Prostate* 2004; **60**: 98–108.
39. Jia G, Zhan Y, Wu D, Meng Y, Xu L. An improved ultrasound-assisted extraction process of gossypol acetic acid from cottonseed soapstock. *AIChE J* 2009; **55**: 797–806.
40. Ji Q, Hao X, Zhang M, Tang W, Yang M, Li L *et al*. MicroRNA miR-34 inhibits human pancreatic cancer tumor-initiating cells. *PLoS One* 2009; **4**: e6816.

Supplementary Information accompanies the paper on Cell Death and Differentiation website (<http://www.nature.com/cdd>)